EPJ Web of Conferences **276**, 02017 (2023) https://doi.org/10.1051/epjconf/202327602017
SQM 2022

Understanding mass hierarchy in different energy loss mechanisms through heavy flavor data

Bojana Ilic[1,*] and *Magdalena* Djordjevic[1]

[1]Institute of Physics Belgrade, University of Belgrade, Belgrade, Serbia

Abstract. The theoretical analysis of experimental observations, such as the mass hierarchy effect, often neglects some ingredients, which may have a significant impact. The forthcoming measurements at RHIC and LHC will generate heavy flavor data with unprecedented precision, providing an opportunity to utilize high-$p_\perp$ heavy flavor data to analyze the interaction mechanisms in QGP. To this end, we use our recently developed DREENA framework based on the dynamical energy loss formalism. We present: i) How to disentangle the signature of different interaction mechanisms (radiative and collisional energy losses) at the same dataset. ii) Novel observables susceptible to these different mechanisms to be tested by future high-precision measurements. iii) Analytical and numerical extraction of the mass hierarchy effect in energy losses through this observable.

1 Introduction

One of the fundamental properties of parton's energy loss is the flavor dependence, that is, the mass ordering. The experimental observation of suppression mass hierarchy [1] is attributed and analyzed within radiative models [2–5], while collisional interactions are neglected. On the other hand, at the intermediate-$p_\perp$ range ($p_\perp \lesssim 10$ GeV) the collisional energy loss for heavy flavor is comparable to, or even larger, than the radiative energy loss [6–10]. However, neither a direct relation between collisional energy loss and heavy quark mass is established, nor an observable which quantifies this effect. Additionally, the upcoming high-precision RHIC and LHC measurements present an opportunity to utilize high-$p_\perp$ heavy flavor data to study the interaction mechanisms in QGP. Note also that D-mesons suppression is practically indistinguishable [1] from $h^\pm$ R_{AA}, which we will exploit in the first part of this document.

Thus, first, we discuss how nonintuitive suppression patterns can be utilized to qualitatively disentangle collisional interaction from radiative energy loss mechanism on the same dataset. In the second part, we focus on the lower-$p_\perp$ range (below 50 GeV) and present: A pursuit for an observable, which could unravel collisional interactions from radiative energy loss. And finally, analytical and numerical extraction of the mass ordering effect in collisional energy loss (for the first time) through this observable, to be more rigorously tested by the upcoming high-luminosity measurements. Note that, in this document, only the main results are displayed, while for more details on the first and second parts, we refer the reader to [4] and [11], respectively.

*e-mail: bojanab@ipb.ac.rs

2 Methods

We employ our full-fledged DREENA-C framework [12], which is based on our state-of-the-art dynamical energy loss formalism [13] (for more details on the model and its reliability see [11]). It also assumes a medium modeled with a constant average temperature. We here choose DREENA-C instead of hydrodynamically-wise more sophisticated versions of DREENA-B or -A [14], to exclude complications originating from details of medium evolution and thus, to provide analytical tractability. This can be achieved without significant loss of accuracy, as we already showed [12, 14, 15] that energy loss-sensitive observable R_{AA} (considered here) is barely sensitive to the medium evolution model. Therefore, DREENA-C provides an optimal framework for these studies, through observable R_{AA}, as it assumes a state-of-the-art energy loss model.

3 Results

In the first part of this paper, we address experimentally observed non-intuitive suppression patterns for both: light or D probes as well as heavy B probes. For light probes (upper left plot of Fig. 1) we see that R_{AA} as a function of N_{part} curves become flatter with increasing $p_\perp$, and that the difference between the curves decreases with increasing $p_\perp$. We call this effect saturation in R_{AA} vs. N_{part} curves. From the lower left plot of Fig. 1, we see flattening of R_{AA} at very high $p_\perp$, to which we refer to as saturation in R_{AA} vs. $p_\perp$ dependence.

Experimental measurements show qualitatively different R_{AA} vs. N_{part} pattern for B probes, compared to the light ones in the upper right plot of Fig. 1. Namely, for two opposite momentum ranges (purple stars vs. blue triangles) the experimental data are practically overlapping. Moreover, R_{AA} vs. N_{part} is flatter across the entire $p_\perp$ range, all of this indicating the saturation of this observable, not only at high $p_\perp$. Measurements of R_{AA} vs. $p_\perp$ (in lower right panel of Fig. 1) display slower change with $p_\perp$ compared to light probes. All these experimental observations are in good agreement with our DREENA-C predictions. So, the question is: which energy loss mechanism is responsible for the observations from Fig. 1?

To qualitatively explain the observations for light or D probes, in Fig. 2 we provide predictions for total (i.e., radiative plus collisional), only collisional, and only radiative R_{AA} vs. $p_\perp$, for a family of curves corresponding to different centralities. The equidistant in $p_\perp$ arrows (at 10, 100, and 190 GeV) indicate the density changes of these curves. From the left plots in first and second rows of Fig. 2, we observe that the leftmost arrow (at lower $p_\perp$) spans a much larger total R_{AA} range compared to the remaining two arrows (at higher $p_\perp$) and which are of a similar span. This explains much steeper R_{AA} vs. N_{part} curves at lower $p_\perp$, and their saturation with increasing $p_\perp$. From the central and right plots in first and second rows of Fig. 2, we see that collisional contribution is only important at lower $p_\perp$, where it increases steeply, while radiative contribution is significant across the entire $p_\perp$ range, but increases slowly. Consequently, the interplay between collisional and radiative contributions is responsible for R_{AA} vs. $p_\perp$ pattern, where steep R_{AA} increase is due to collisional, while saturation is due to radiative contributions.

Regarding B, mostly uniform R_{AA} vs. $p_\perp$ curves' density across the entire $p_\perp$ range (left plot in third row of Fig. 2) results in R_{AA} vs. N_{part} curves' overlap regardless of $p_\perp$. Central and right plots in the third row of Fig. 2 indicate that at lower $p_\perp$ both collisional and radiative contributions are important but significantly smaller than for light probes. Consequently, the mass hierarchy in collisional and radiative energy losses are responsible for R_{AA} vs. $p_\perp$ shape at lower $p_\perp$, while the flat radiative contribution plays a decisive role at higher $p_\perp$.

In the second part of this paper, we dive deeper into energy loss mechanisms and focus on the $p_\perp \lesssim 50$ GeV region. First, by comparing DREENA-C patterns in energy losses of charm

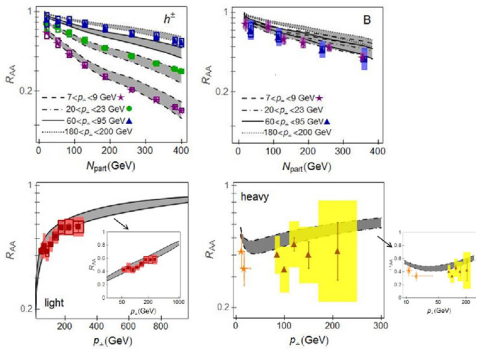

Figure 1. Comparison of suppression patterns data and predictions (gray bands) for light (left column) and B-probes (right column). For experimental data see [4]. Figure adapted from [4].

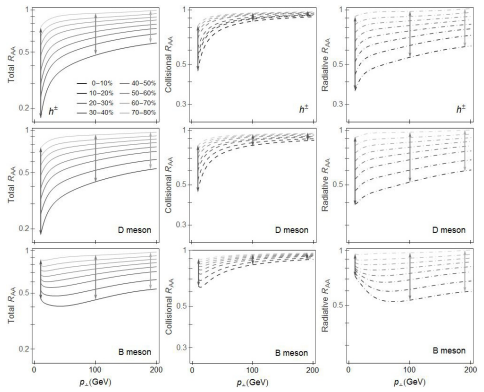

Figure 2. Explanation of suppression patterns for light (upper), D (middle) and B (lower row) probes. Left, central and right plots show, respectively, total, collisional and radiative R_{AA}. Figure adapted from [4].

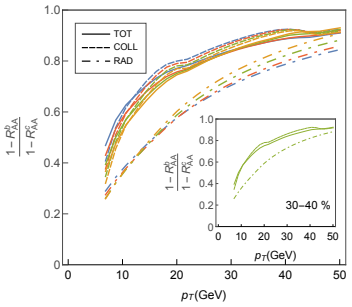

Figure 3. DREENA-C $(1 - R^b_{AA})/(1 - R^c_{AA})$ total (full), collisional (dashed) and radiative (dot-dashed curves) cases for centralities (as in Fig. 4 legend) are displayed. For clarity, 30 – 40% centrality is singled out. Figure adapted from [11].

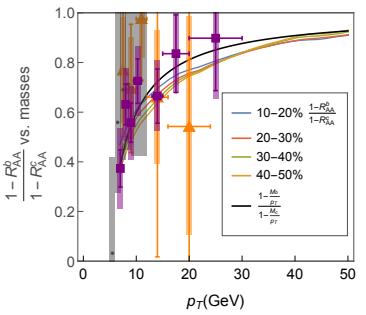

Figure 4. Numerical verification of $(1-R^b_{AA})/(1-R^c_{AA})$ as an adequate observable for mass extraction from collisional contribution, through comparison with experimental data (for more details see [11]. Figure adapted from [11].

and bottom (see Fig. 1 from [11]) we observe that we reproduced the dead-cone effect [16] in radiative energy loss, and clear mass ordering in $\Delta E_{coll}/E$ also. Compared to the $\Delta E_{rad}/E$, this effect in $\Delta E_{coll}/E$ is slightly less pronounced, but it is a significant observation. The question is, which observable could quantify this effect? To this end, we recall [11] that it should be a function of high-$p_\perp$ $1 - R_{AA}$, since it carries explicit information on the parton's energy loss [15, 17] while being practically insensitive to the details of medium evolution.

Guided by this idea, in Fig. 3 we compare $1-R_{AA}$ bottom to charm ratios (for different centralities), when only collisional, only radiative, and total interactions are considered. Surprisingly, we find that $(1-R^{b,tot}_{AA})/(1-R^{c,tot}_{AA})$ is essentially overlapping with $(1-R^{b,coll}_{AA})/(1-R^{c,coll}_{AA})$, which is true for all centralities. This is a nontrivial and significant insight. Consequently, Fig. 3 shows that collisional contribution is in the origin of $(1 - R^{b,tot}_{AA})/(1 - R^{c,tot}_{AA})$. Thus, in paper [11] we proposed $(1 - R^b_{AA})/(1 - R^c_{AA})$ as a new observable which may quantify

the mass hierarchy in collisional energy loss. Moreover, after some algebraic manipulations (for more details see [11]), where collisional suppression definition [10, 18] as well as mass parameterization of heavy quarks initial distribution is applied [19], we infer that the $(1-R^b_{AA})/(1-R^c_{AA}) \simeq (1-\frac{M_b}{p_\perp})/(1-\frac{M_c}{p_\perp})$ reflects the mass hierarchy in collisional energy loss. This provides analytical support to $(1-R^b_{AA})/(1-R^c_{AA})$ as the appropriate new observable.

Furthermore, we get that $(1-R^b_{AA})/(1-R^c_{AA})$ is robust to the collision centrality (see Fig. 3), collision system, and collision energy (see Fig. 4). Therefore, we propose that the new observable should have general applicability to both the RHIC and the LHC experiments, independently of collision centrality, as long as QGP is formed.

4 Conclusions and outlook

Complex and significantly different suppression patterns for different flavors inspired us to distinguish between radiative and collisional contributions at the same dataset. Then, focused on the $p_\perp \lesssim 50$ GeV range, where both energy loss mechanisms are important for heavy probes, we proposed an observable, which could disentangle collisional from radiative energy loss. Also, by comparing with scarce heavy flavor data, we numerically verified the adequacy of the proposed observable for extracting mass hierarchy from collisional energy loss.

As an outlook, our analysis provides specific guidelines for future experiments. For instance, regarding non-intuitive suppression patterns, efforts should be concentrated on single-particle measurements to much higher $p_\perp$, while regarding the new observable, at the lower $p_\perp$ region, which is accessible at both RHIC and LHC. Note that current error bars are still large, so we expect that the upcoming high-luminosity measurements will provide a more rigorous test for this new observable. Finally, the suppression measurements of both b and c probes in the same centrality bins would be highly useful.

References

[1] A. M. Sirunyan *et al.* [CMS], Phys. Rev. Lett. **123**, no.2, 022001 (2019)
[2] N. Armesto, C. A. Salgado and U. A. Wiedemann, Phys. Rev. D **69**, 114003 (2004)
[3] M. Djordjevic and U. Heinz, Phys. Rev. C **77**, 024905 (2008)
[4] M. Djordjevic, Phys. Lett. B **763**, 439-444 (2016)
[5] B. W. Zhang, E. Wang and X. N. Wang, Phys. Rev. Lett. **93**, 072301 (2004)
[6] S. Wicks, W. Horowitz, M. Djordjevic and M. Gyulassy, Nucl. Phys. A **784**, 426 (2007)
[7] M. Djordjevic, Phys. Rev. C **74**, 064907 (2006)
[8] B. Blagojevic and M. Djordjevic, J. Phys. G **42**, no.7, 075105 (2015)
[9] M. H. Thoma, Phys. Lett. B **273**, 128-132 (1991)
[10] M. G. Mustafa, Phys. Rev. C **72**, 014905 (2005)
[11] Bojana Ilic and Magdalena Djordjevic, Phys. Rev. C **1**06, 014902 (2022)
[12] D. Zigic, I. Salom, J. Auvinen, M. Djordjevic and M. Djordjevic, J. Phys. G **46**, 085101 (2019)
[13] M. Djordjevic and M. Djordjevic, Phys. Lett. B **734**, 286-289 (2014)
[14] D. Zigic, I. Salom, J. Auvinen, M. Djordjevic and M. Djordjevic, Phys. Lett. B **791**, 236-241 (2019); [arXiv:2110.01544 [nucl-th]]
[15] M. Djordjevic, D. Zigic, M. Djordjevic and J. Auvinen, Phys. Rev. C **99**, 061902 (2019)
[16] Y. L. Dokshitzer and D. E. Kharzeev, Phys. Lett. B **519**, 199-206 (2001)
[17] S. Stojku, B. Ilic, M. Djordjevic and M. Djordjevic, Phys. Rev. C **103**, 024908 (2021)
[18] M. H. Thoma and M. Gyulassy, Nucl. Phys. B **351**, 491-506 (1991)
[19] G. D. Moore and D. Teaney, Phys. Rev. C **71**, 064904 (2005)